AMERICAN SOCIETY FOR MICROBIOLOGY | Journal of Virology®

VIRUS-CELL INTERACTIONS

Novel Host Recognition Mechanism of the K1 Capsule-Specific Phage of *Escherichia coli*: Capsular Polysaccharide as the First Receptor and Lipopolysaccharide as the Secondary Receptor

Qianwen Gong,[a] Xuhang Wang,[a] Haosheng Huang,[a] Yu Sun,[a] Xinjie Qian,[a] Feng Xue,[a] Jianluan Ren,[a] Jianjun Dai,[a,b] Fang Tang[a]

[a]MOE Joint International Research Laboratory of Animal Health and Food Safety; Key Laboratory of Animal Bacteriology, Ministry of Agriculture; and College of Veterinary Medicine, Nanjing Agricultural University, Nanjing, China

[b]School of Life Science and Technology, China Pharmaceutical University, Nanjing, China

ABSTRACT K1 capsule-specific phages of *Escherichia coli* have been reported in recent years, but the molecular mechanism involved in host recognition of these phages remains unknown. In this study, the interactions between PNJ1809-36, a new K1-specific phage, and its host bacterium, *E. coli* DE058, were investigated. A transposon mutation library was used to screen for receptor-related genes. Gene deletion, lysis curve determination, plaque formation test, adsorption assay, and inhibition assay of phage by lipopolysaccharide (LPS) showed that capsular polysaccharide (CPS) was the first receptor for the initial adsorption of PNJ1809-36 to *E. coli* DE058 and that LPS was a secondary receptor for the irreversible binding of the phage. The penultimate galactose in the outer core was identified as the specific binding region on LPS. Through antibody blocking assay, fluorescence labeling and high-performance gel permeation chromatography, the tail protein ORF261 of phage PNJ1809-36 was identified as the receptor-binding protein on CPS. Given these findings, we propose a model for the recognition process of phage PNJ1809-36 on *E. coli* DE058: the phage PNJ1809-36 tail protein ORF261 recognizes and adsorbs to the K1 capsule, and then the K1 capsule is partially degraded, exposing the active site of LPS which is recognized by phage PNJ1809-36. This model provides insight into the molecular mechanisms between K1-specific phages and their host bacteria.

IMPORTANCE It has been speculated that CPS is the main receptor of K1-specific phages belonging to *Siphoviridae*. In recent years, a new type of K1-specific phage belonging to *Myoviridae* has been reported, but its host recognition mechanisms remain unknown. Here, we studied the interactions between PNJ1809-36, a new type of K1 phage, and its host bacterium, *E. coli* DE058. Our research showed that the phage initially adsorbed to the K1 capsule mediated by ORF261 and then bound to the penultimate galactose of LPS to begin the infection process.

KEYWORDS phage, *Escherichia coli*, receptor, LPS, K1 capsule

Phages are natural viral bacterial predators. The total number of global phages is estimated at roughly 10^{31} phage particles, making them the most abundant microorganisms in the biosphere. Due to the increasing drug resistance of bacteria, phage therapy is now experiencing a renaissance (1). One of the biggest problems with phage therapy is that bacteria can quickly become resistant to phages. The resistance is often related to the fact that the phage cannot recognize the host bacteria due to the mutation of receptors on the surface of the host cell. Therefore, it is critical to study the mechanisms by which phages interact with their host receptors (2). Phages recognize host bacteria by interactions between host-encoded receptors and phage-encoded receptor-binding proteins (RBPs) (3). Phage adsorb to bacteria via various receptors on the surface of the hosts, which range from peptide sequences to polysaccharide moieties, including proteins, lipopolysaccharide (LPS) and

Citation Gong Q, Wang X, Huang H, Sun Y, Qian X, Xue F, Ren J, Dai J, Tang F. 2021. Novel host recognition mechanism of the K1 capsule-specific phage of *Escherichia coli*: capsular polysaccharide as the first receptor and lipopolysaccharide as the secondary receptor. J Virol 95:e00920-21. https://doi.org/10.1128/JVI.00920-21.

Editor Julie K. Pfeiffer, University of Texas Southwestern Medical Center

Address correspondence to Fang Tang, tfalice@126.com.

Received 4 June 2021
Accepted 15 June 2021
Accepted manuscript posted online 30 June 2021
Published 25 August 2021

carbohydrate moieties (4). In Gram-negative bacteria, in addition to outer membrane proteins, pili, and flagella, LPS is a common receptor for phages (5). LPS of *Escherichia coli* can be classified into five types according to the structure of the outer core regions: R1, R2, R3, R4, and K-12 (6). The mechanisms of phage recognizing different types of LPS are different. The gene cluster of *waa* (*rfa*) encodes a variety of glycosyltransferases that assist in forming the LPS polysaccharide core, such as *waaO*, *waaT*, and others. Usually in such studies, these genes are knocked out to form different LPS mutants to identify the binding region of phage to LPS (7). For example, T4 was identified to bind to a specific LPS with only one (Glc I) or two glucoses (Glc I and Glc II) in the outer core of K-12 LPS through construction of deletion mutants; by knocking out genes of the *waa* gene cluster, it was found that the LPS binding region of phage VpaE1 to strain BW25113 (a K-12 type of LPS) was the inner core residue (8). Among the studies of interactions between phage and LPS, the recognition mechanism of phages on the LPS type of K-12 (*E. coli* K-12) and on defective R1 (*E. coli B*) have been the most well investigated. For example, the phages Mu(+) and ST-1 adsorb to *E. coli* K-12 LPS on terminal Glcα-2Glcα1 and GlcNAcα1-2Glcα1 of LPS, respectively (9). Both T4 and T3 adsorb *E. coli B* on the glucosyl-α-1,3-glucose terminus of LPS (7, 10). However, the mechanisms of how phage adsorb to *E. coli* with R1 LPS remains unclear.

The capsule is one of the important virulence factors as well as a crucial antigen in *E. coli* (11). The components of the capsule are mainly extracellular polysaccharides. K1 capsule is considered to be the main pathogenic factor of *E. coli* that can cross the blood-brain barrier and cause neonatal meningitis (12). In addition, the capsule can also be recognized as a receptor by phages (13, 14). A variety of phages with polysaccharide specificity have been isolated. Among them, K1-dependent phage can degrade polysialic acid (PSA) in the K1 capsule specifically, thus weakening its pathogenicity (15). In earlier reports, most K1-dependent phages were *Siphoviridae* or *Podoviridae*, such as 63D (16), K1E and K1F (17, 18). Some phages can use capsular polysaccharides (CPS) as primary receptors, and they usually have virion-bound depolymerization enzymes which degrade polysaccharides and help the phage reach the surface of the bacteria (19). K1E and K1F were found to encode a tail protein having endo-*N*-acetylneuraminidase activity that can degrade the K1 capsule, which was observed by immunoelectron microscopy (20). In the last decade, new phages with contractile tails sharing low homology to K1E and K1F have been discovered, such as *Salmonella* phage PVP-SE1 (isolated in 2011), *E. coli* phage phAPEC8 (in 2010), ESCO5 and ESCO13 (in 2019), nepoznato (in 2017), and others (21–23). These phages share some homology with K1E and K1F endo-*N*-acetylneuraminidase, so it has been speculated that their adsorption process is related to K1, but this lacks experimental validation.

In our previous work, phage PNJ1809-36 (accession number MT944117) with a contractile tail was isolated from chicken feces. It specifically infected *E. coli* with the K1 capsule. The optimal multiplicity of infection (MOI) of phage PNJ1809-36 was 0.01. The latent period was 10 min, and the burst size was 122. The size of the phage genome is 152,343 bp, with 277 predicted open reading frames (ORFs) and 11 tRNA genes. The genome analysis showed that phage PNJ1809-36 had low sequence identity with earlier-reported *E. coli* K1-specific phages, such as K1F and K1E, but shared high sequence homology with phages nepoznato, PVP-SE1 and phAPEC8, with highest homology with phAPEC8 (98%) (24). However, the mechanism of host recognition by these phages to K1 *E. coli* remains unknown. The host bacterium DE058 is an *E. coli* strain harboring the K1 capsule and R1 LPS. In the present study, we identified CPS and LPS as receptors of phage PNJ1809-36. The tail proteins of phage binding to CPS were also confirmed.

RESULTS

***E. coli* DE058 is identified as possessing the K1 capsule and R1 LPS.** The genomic size of *E. coli* DE058 (accession number JACRRZ000000000) was 5,001,854 bp, with GC content of 50.62%. A total of 4,774 genes were predicted, including 4,695 coding sequences, 4 rRNA, and 74 tRNAs. In our previous study, we identified the K1 capsule by PCR (24). According to previous publications (25), the K1 capsule gene cluster is divided into three regions, of which region 2 is the specific central region, and region 1 or 3 is the conserved region (Fig. 1A). The

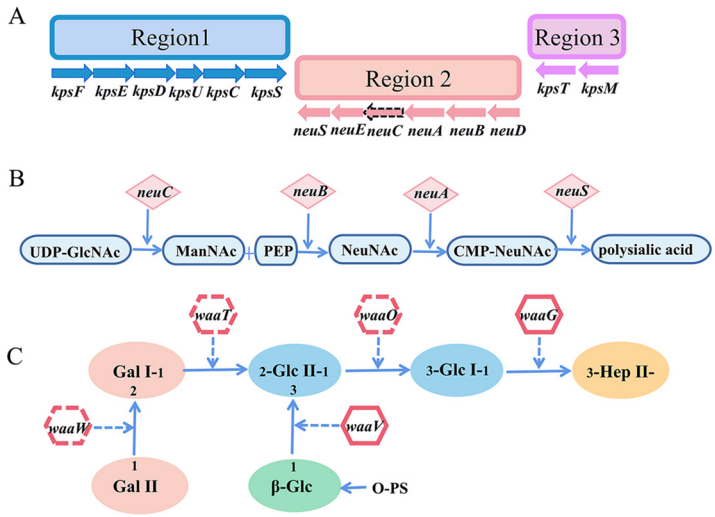

FIG 1 Gene cluster diagram of the outer core polysaccharides of R1 LPS and K1 capsule. (A) K1 capsular conserved gene cluster of DE058. The dotted line represents the deleted gene *neuC*. (B) Synthesis of *N*-acetylneuraminic acid in the K1 capsule and site of the enzyme encoded by each gene. (C) Schematic diagram of the synthesis process of outer core polysaccharides of LPS. Different colors represent different oligosaccharides. The solid arrow represents the direction of outer core polysaccharide synthesis. Dotted arrows represent the sites at which different transferases act, adding different oligosaccharides to the outer core polysaccharide chain.

genes in region 2 promote formation of sialic acid monomers by expressing various enzymes (Fig. 1B) which polymerize PSA as the K1 capsule main component. The LPS structure of DE058 was identified as R1 by BLAST (6) and was formed with the help of the transferase encoded by the *waa* gene cluster (Fig. 1C).

***waaO*, *waaT*, and *neuC* are involved in phage infection.** A random transposon insertion mutant library was constructed from *E. coli* DE058 to identify phage receptor-associated genes. Phage-resistant mutant strains were selected by monitoring the decrease in optical density at 600 nm (OD_{600}) when cocultured with phage PNJ1809-36 and by assessing the number of plaques in double-layer agar. Of ~14,000 insertion mutants, 15 phage-resistant mutants were selected. DNA sequencing of the region flanking the insertions in the 15 mutants revealed nine insertions in gene *waaO*, five insertions in gene *waaT* and one insertion in gene *neuC* (Table 1). *waaO* and *waaT* are annotated as glycosyltransferases in the synthesis of LPS, while *neuC* is related to CPS synthesis. Mutants associated with *waaO* and *waaT* insertions were completely resistant to phage PNJ1809-36, with no plaques in double-layer agar, while mutants with the *neuC* insertion were not completely resistant to phage PNJ1809-36, producing a vague and opaque clearing in spot assays (Fig. 2). Gene deletion mutants were also constructed and tested for phage susceptibility. As expected, the Δ*waaO* and Δ*waaT* mutants were completely resistant to phage PNJ1809-36, while the Δ*neuC* mutant was partially resistant to phage PNJ1809-36, consistent with the phenotype of Tn5 insertion mutants. All the complementary strains recovered sensitivity to PNJ1809-36.

CPS is the preliminary adsorption receptor. We analyzed the synthesis of LPS- and CPS-associated sequences of DE058. *neuC* encodes UDP-*N*-acetylglucosamine 2-epimerase, which carries out the reversible epimerization of UDP-GlcNAc to ManNAc. We hypothesized that deletion of the *neuC* gene abolishes synthesis of ManNAc and interrupts the synthesis of sialic acid monomers (26), which are the main component of CPS, thus preventing phage adsorption to host bacteria. To verify this, the phage adsorption rates of the wild type (WT), gene deletion mutants, and complementary strains were determined. The Δ*neuC* strain had a 45% decrease in phage adsorption rate (Fig. 3A). This indicated that the integrity of CPS was important for the adsorption. In accordance with the above results, when observed by electron microscopy, the WT and complementary strains were rough, with more extracellular polysaccharides on the surface, whereas the Δ*neuC* mutant was smooth (Fig. 3B). Capsule staining results also showed that the capsule was present in the

TABLE 1 Bacterial strains and plasmids

Strain or plasmid	Relevant characteristics	Source or reference
Strains		
E. coli		
DH5α	F$^-$ Δ(*lacZYA-argF*)*U169 recA1 endA1 hsdR17*(r_K^- m_K^+) *phoA supE44* λ^-	Vazyme
BL21(DE3)	F$^-$ *ompT hsdS*(r_B^- mB^-) *gal dcm* (DE3)	Vazyme
S17-1λpir	Put-Mini-Tn5-Km Amp^r Km^r	Zhe Ma, Nanjing Agricultural University
DE058	Wild-type strain-Amp^s Km^s K1	This study (A_0 in Fig. 2)
17-4F	DE058-Tn5-*waaO*(*rfaJ*) Nal^r Km^r	This study (A_1 in Fig. 2)
39-5A	DE058-Tn5-*waaO*(*rfaJ*) Nal^r Km^r	This study (A_2 in Fig. 2)
39-6B	DE058-Tn5-*waaO*(*rfaJ*) Nal^r Km^r	This study (A_3 in Fig. 2)
39-9B	DE058-Tn5-*waaO*(*rfaJ*) Nal^r Km^r	This study (A_4 in Fig. 2)
41-1B	DE058-Tn5-*waaO*(*rfaJ*) Nal^r Km^r	This study (A_5 in Fig. 2)
48-1A	DE058-Tn5-*waaT*(*F3J96-24975*) Nal^r Km^r	This study (A_6 in Fig. 2)
49-3E	DE058-Tn5-*waaO*(*rfaJ*) Nal^r Km^r	This study (A_7 in Fig. 2)
85-6F	DE058-Tn5-*neuC* Nal^r Km^r	This study (A_8 in Fig. 2)
73-4F	DE058-Tn5-*waaT*(*F3J96-24975*) Nal^r Km^r	This study (A_9 in Fig. 2)
78-11E	DE058-Tn5-*waaT* (*F3J96-24975*) Nal^r Km^r	This study (A_{10} in Fig. 2)
81-1E	DE058-Tn5-*waaT*(*F3J96-24975*) Nal^r Km^r	This study (A_{11} in Fig. 2)
63-6E	DE058-Tn5-*waaO* (*rfaJ*) Nal^r Km^r	This study (A_{12} in Fig. 2)
93-1F	DE058-Tn5-*waaT*(*F3J96-24975*) Nal^r Km^r	This study (A_{13} in Fig. 2)
113-12G	DE058-Tn5-*waaO*(*rfaJ*) Nal^r Km^r	This study (A_{14} in Fig. 2)
123-8H	DE058-Tn5-*waaO*(*rfaJ*) Nal^r Km^r	This study (A_{15} in Fig. 2)
Δ*waaO*	Deletion of *waaO* from DE058	This study
C-Δ*waaO*	Δ*waaO*-pSTV28-*waaO*	This study
Δ*waaT*	Deletion of *waaT* from DE058	This study
C-Δ*waaT*	Δ*waaT*-pSTV28-*waaT*	This study
Δ*neuC*	Deletion of *neuC* from DE058	This study
C-Δ*neuC′*	Δ*neuC*-pSTV28-*neuC*	This study
Δ*waaW*	Deletion of *waaW* from DE058	This study
C-Δ*waaW*	Δ*waaW*-pSTV28-*waaW*	This study
Phage		
PN1809-36	*E. coli* phage	This study
Plasmids		
pKD46	Amp; expresses λ red recombinase	43
pKD4	*kan* gene, template plasmid	43
Pcp20	Cm, Amp, yeast Flp recombinase gene, FLP	43
pSTV28	Cm, *lacZ*	Takara
pSTV28-*waaO*	pSTV28 derivative harboring *waaO* ORF and its putative promoter	This study
pSTV28-*waaT*	pSTV28 derivative harboring *waaT* ORF and its putative promoter	This study
pSTV28-*neuC*	pSTV28 derivative harboring *neuC* ORF and its putative promoter	This study
pET28a(+)	Kan, F1 origin, His tag	Novagen

WT and the complementary strain (C-*neuC*), but not in the Δ*neuC* mutant strain (Fig. 3B). In addition, fuzzy clearings appeared with the Δ*neuC* strain (Fig. 3C), which suggested that the Δ*neuC* strain could not be completely lysed by phage. The phage lysis curve *in vitro* was also consistent with this finding (Fig. 3D). These results suggest that CPS plays an important role in the initial stage of phage adsorption to bacteria.

LPS is the secondary binding receptor. *waaO* encodes the LPS α-1,3-glucosyltransferase for the α-(1-3)-linked Glc residue. *waaT* is translated into LPS α-1,2-galactosyltransferase for the α-(1-2)-linked Gal residue, and *waaW* is translated into LPS α-1,2-galactosyltransferase for the terminal α-(1-2)-linked Gal residue (6) (Fig. 1C). Thus, the deletion of *waaO* or *waaT* switched off the linking of Glc or Gal residues, which led to a structural change in the outer core polysaccharides of LPS. Unlike the Δ*neuC* strain, the Δ*waaO* and Δ*waaT* mutants showed a slight decrease in the phage adsorption rate and could completely block infection by phage, which suggests that further receptors may be involved (Fig. 4A). To further verify the necessity of LPS as a binding receptor during phage infection, adsorption inhibitor experiments were performed using LPS extracted from DE058. The plaque formation rate of phage PNJ1809-36 was negatively

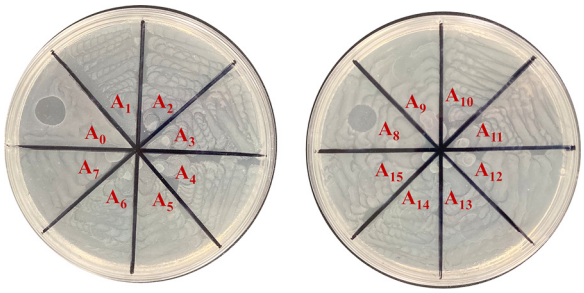

FIG 2 Spotting the phage-resistant strains from the mutant library. Fifteen phage-resistant mutants selected through monitoring OD_{600} values were used for spotting in the second screening assay. A0 was the control (DE058), and A1 to A15 were the mutants.

correlated with the amount of added LPS (Fig. 4B), indicating that LPS could inhibit phage infection. Δ*waaO* and Δ*waaT* strains were phage resistant (Fig. 4C, D, F, and G), indicating that Gal I and Gal II may be binding regions. To further identify the exact binding region in LPS, *waaW* was knocked out. The sensitivity of the Δ*waaW* mutant to phage was similar to WT (Fig. 4E and H), suggesting that the exact binding region of phage PNJ1809-36 on DE058 LPS was the penultimate galactose Gal I (Fig. 4E). LPS had little effect on adsorption but had a large effect on plaque formation, indicating that it was the second receptor. To further detect whether there were any protein receptors on DE058, the bacteria were treated with proteinase K or periodate. The results showed that there was very little difference in the adsorption rate between proteinase

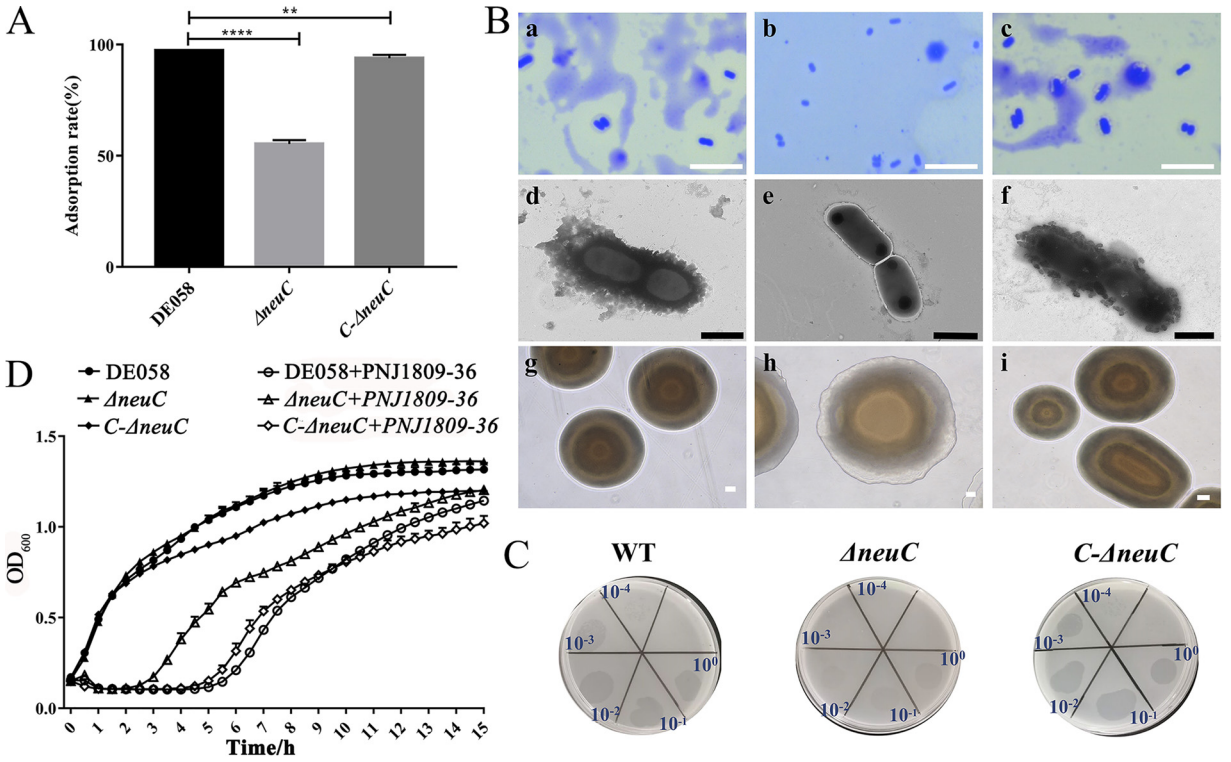

FIG 3 CPS acts as the adsorption receptor. (A) Adsorption assay. The number of free phages was detected after the adsorption of DE058 (WT), Δ*neuC*, and C-Δ*neuC* strains for 10 min, and the adsorption rate of the WT strain was set at 100%. Means with standard deviations from triplicate experiments are shown. **, $P < 0.01$; ****, $P < 0.0001$. (B) Capsule morphology. (Subpanels a to j) Capsule staining figures of WT (a), Δ*neuC* (b), and C-Δ*neuC* strains (c); electron microscopic picture of WT (d), Δ*neuC* (e), and C-Δ*neuC* strains (f); and colony morphology of WT (g), Δ*neuC* (h), and C-Δ*neuC* strains (i). Scale bars: 10 μm (a to c), 1 μm (d to f), and 100 μm (g to i). (C) Plaque assay showing clear plaque on the WT and C-Δ*neuC* strains and fuzzy clearing on the Δ*neuC* strain. (D) Lysis curves for WT, Δ*neuC*, and C-Δ*neuC* strains.

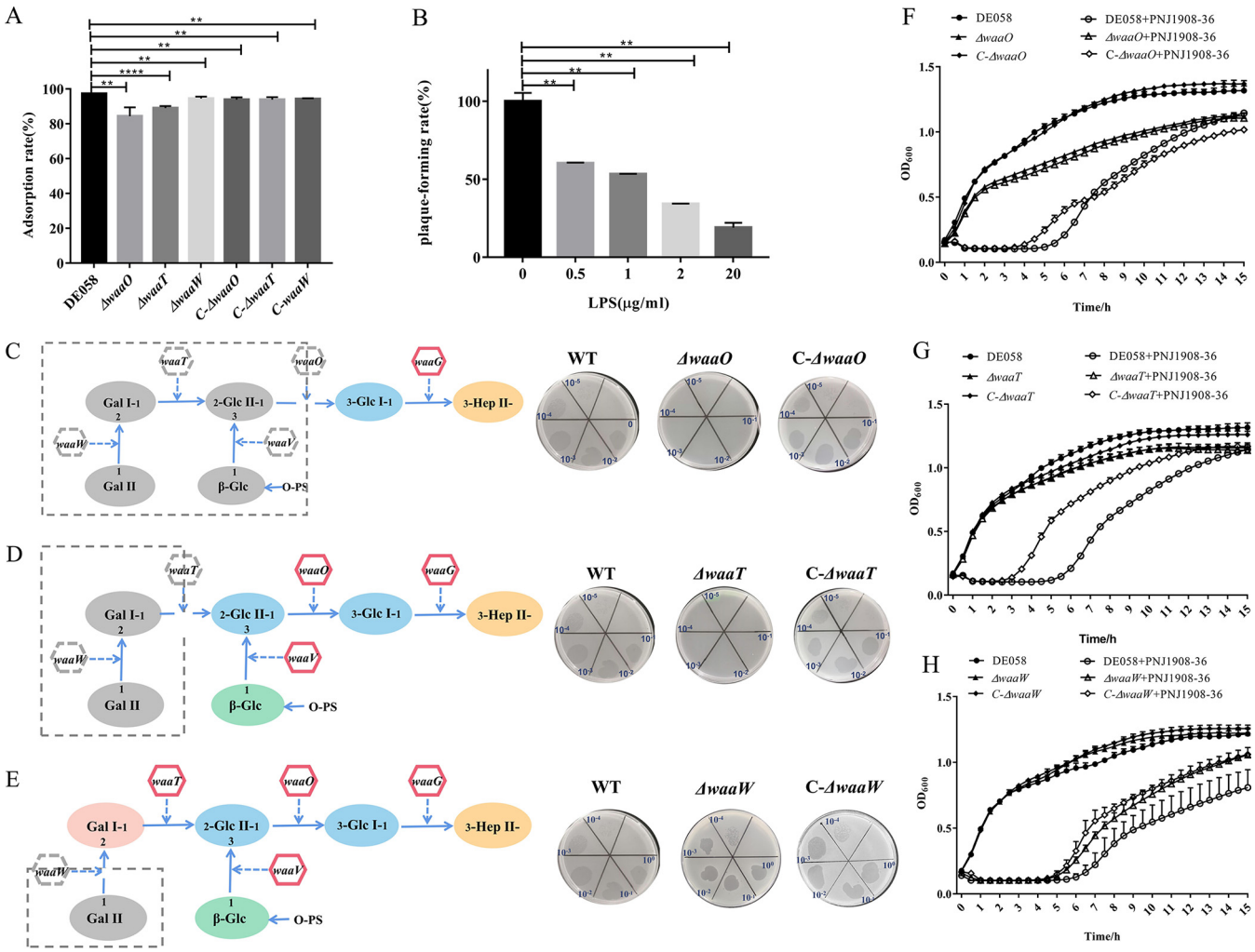

FIG 4 LPS is the binding receptor. (A) The adsorption rates of LPS-related gene deletion and complementary strains (Δ*waaO*, C-Δ*waaO*, Δ*waaT*, C-Δ*waaT*, Δ*waaW*, and C-Δ*waaW*) were measured to compare with DE058, and the adsorption rate of the WT strain was set at 100%. All assays were performed in triplicate. **, $P < 0.05$; ****, $P < 0.0001$. (B) LPS was added to compete for LPS receptor *in vitro*. After the addition of different concentrations of LPS from DE058 *in vitro*, plaque-forming ability with DE058 host bacteria was detected. **, $P < 0.01$; ****, $P < 0.0001$. (C to E) LPS structure and spot formation of gene deletion mutants. The gray box represents the deleted portion, and the remaining is truncated LPS. The right panels show plaque formation of WT, deletion, and complementary strains (*waaO*, *waaT*, and *waaW*). (F) Lysis curve of WT, Δ*waaO*, and C-Δ*waaO* strains. (G) Lysis curve of WT, *waaT*, and C-Δ*waaT* strains. (H) Lysis curve of WT, Δ*waaW*, and C-Δ*waaW* strains.

K-treated DE058 and the untreated control group (Fig. 5A), but the adsorption rate was decreased with the increase in periodate concentration (Fig. 5B), indicating that there was no protein receptor for phage PNJ1809-36 on DE058, while destruction of the polysaccharide receptor hampered the adsorption process.

ORF261 of phage specifically binds to CPS. Next, we tried to identify the phage-encoded receptor-binding proteins (RBPs). ORF261 of PNJ1809-36 shared 99% homology with the protein (sequence ID YP_007348539.1) of phAPEC8 in protein sequence (Fig. 6) and shared 74% amino acid identity with the endo-*N*-acetylneuraminidase of the K1-dependent phages K1G (accession number GU196277.1) and K1H (accession number GU196278.1) (22). However, the function of this protein has not been previously studied. The tail protein ORF261 of PNJ1809-36 was predicted to be an endo-*N*-acetylneuraminidase which can bind and decompose polyneuraminic acid (K1 capsule). Therefore, the recombinant protein ORF261 was constructed and purified. We found that when the phage PNJ1809-36 was pretreated with polyclonal antibody against ORF261, the titer of free phages decreased by 95.8% compared to the titer of phages pretreated with anti-ORF249 (Fig. 7A), and the results of competition assays showed that the adsorption rate decreased by 40.6% after DE058 was blocked by

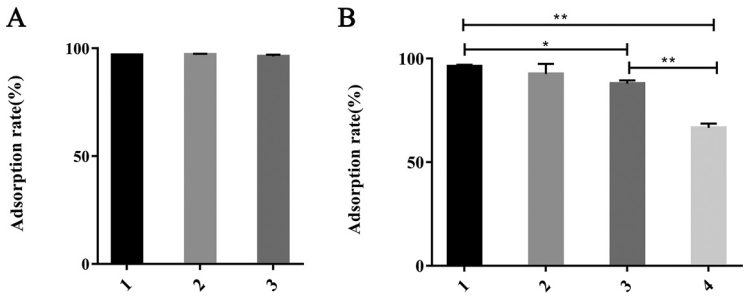

FIG 5 Adsorption rate of phage PNJ1809-36 to host DE058 treated with different agents. (A) Adsorption rates of the host bacteria treated with proteinase K. Columns 1, 2, and 3 represent the respective added substances: 1, LB medium (negative control); 2, 20 mM Tris-HCl and 100 mM NaCl (pH 7.5); 3, 0.5 mg/ml proteinase K in 20 mM Tris-HCl and 100 mM NaCl (pH 7.5). (B) Adsorption rates of host bacteria treated with periodate. Columns 1, 2, 3, and 4 indicate the addition of different reagents: 1, LB medium (negative control); 2, 50 mM CH_3COONa (pH 5.2); 3, 10 mM sodium periodate ($NaIO_4$) and 50 mM sodium acetate (CH_3COONa) (pH 5.2); 4, 100 mM $NaIO_4$ and 50 mM CH_3COONa (pH 5.2). **, $P < 0.01$.

phage-tail protein ORF261 (Fig. 7B), indicating that ORF261 was one of the RBPs. The binding of protein ORF261 to strain DE058 was further evaluated using epifluorescence microscopy. The protein ORF261-GFP and GFP were expressed and incubated with the WT, the Δ*neuC* mutant strain, and the C-Δ*neuC* complementary strain. As a result, strong green fluorescence was observed in WT and complementary strains but only much fainter green fluorescence was observed in the Δ*neuC* strain. Green fluorescent protein (GFP) alone could not be combined with the WT, Δ*neuC*, or complementary strain (Fig. 7C), indicating that it was ORF261 that bound to CPS of DE058. To further determine whether ORF261 could decompose CPS, high-performance gel permeation chromatography (HPGPC) was performed using PSA as the substrate. The results showed that the molecular weight of the digested product PSA-1 decreased to ~13,018 Da (Fig. 7D) after treatment with a small amount of enzyme ORF261, while the molecular weight of the control group remained at ~91,910 Da, indicating that the PSA was decomposed by protein ORF261.

DISCUSSION

Studying the entire infection process, starting with the adsorption step, can help us to understand phage ecology and accelerate the development of phage-based technologies. During infection, after facilitating attachment to a primary receptor, some phages require a secondary receptor to irreversibly bind to host bacteria. For instance, the long tail fiber of phage T4 reversibly binds to the first receptor, LPS of *E. coli*, which subsequently irreversibly binds to the host's second receptor, the heptose moiety of LPS (27). Phage T5 adsorbs to O-antigen's polymannose moiety in *E. coli* LPS, then irreversibly binds to the outer membrane protein receptor FhuA (28, 29). It was also reported that phage irreversibly adsorbing to the first cell wall-associated moiety makes the second host receptor more exposed and easier to access, increasing the stability and the probability of finding the cell receptor associated with irreversible binding (4). Here, we illustrate a new host recognition mechanism that *Myoviridae* phages utilize to infect *E. coli* by successively recognizing K1 CPS and R1 LPS, which has only been rarely reported.

In this study, *neuC* deletion resulted in disruption of capsule synthesis and further led to a significantly decreased capacity for phage adsorption, suggesting that CPS provides the receptor for phage adsorption. This result is in agreement with some other K1 phages, such as K1F and K1-5 (30). Here, capsule disruption is due to mutation of gene *neuC*.

In addition to genetic mutations, phase-variable expression of CPS has been reported to regulate the sensitivity to phage. For example, in *Bacteroides thetaiotaomicron*, the expression of cps1 and cps4 was significantly decreased, while expression from the nonpermissive cps3 locus was significantly increased after being treated with phage ARB25 (31). Capsular protein can be a receptor recognized by phages, but in some cases, it can physically block the infection of phages such as T7, which recognizes LPS as the primary receptor (30). In

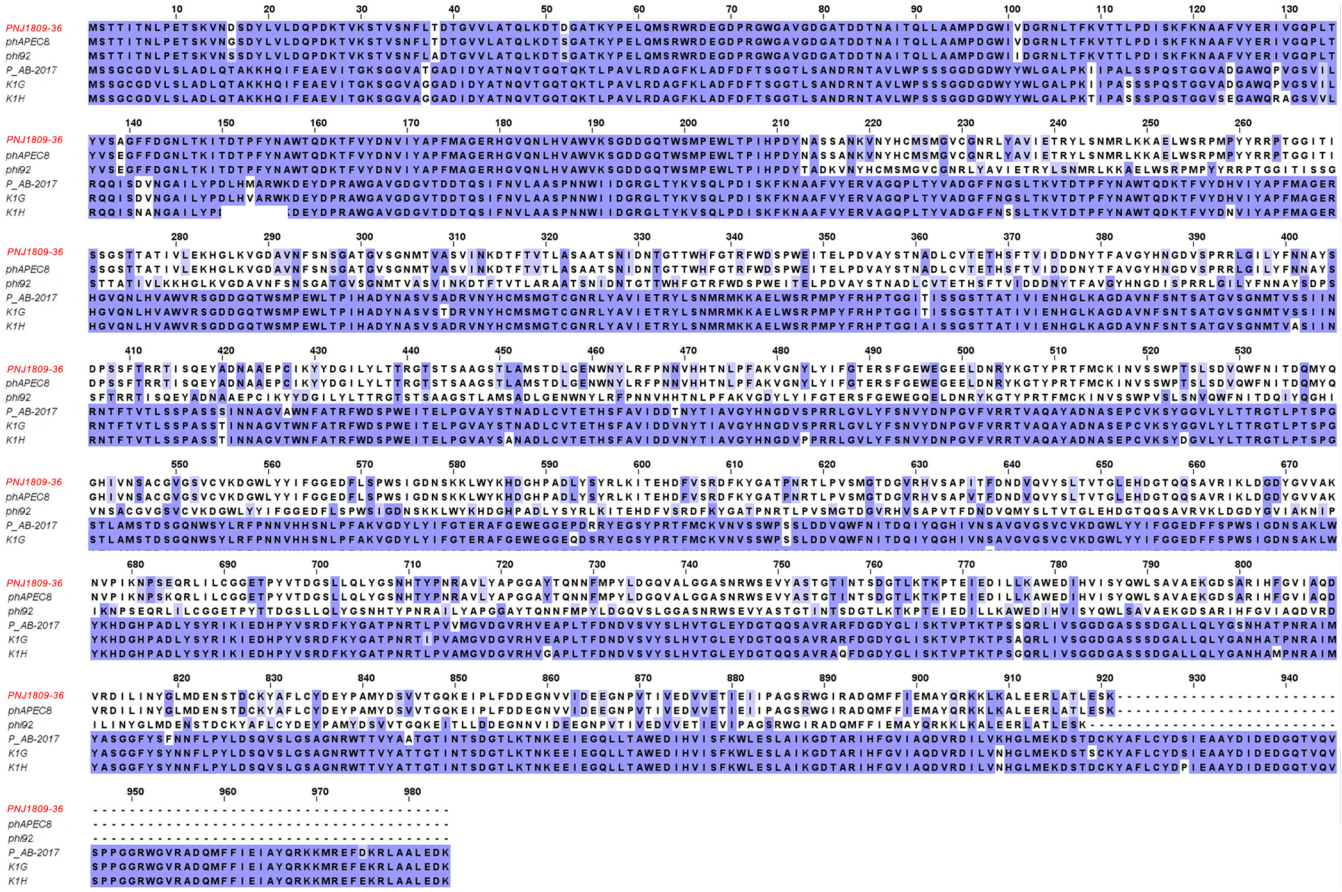

FIG 6 Amino acid sequence alignment of ORF261 and other proteins. ORF261 shares the highest amino acid homology with the tail proteins of phAPEC8 (sequence ID YP_007348539.1) and phi92 (sequence ID YP_009012475.1), and the next highest homology with phage PAB2017 (sequence ID AQN31942.1), K1G (sequence ID YP_009168811.1), and K1H (sequence ID YP_009168860.1).

contrast to T7, our results showed that capsular recognition facilitates phage PNJ1809-36 finding the second LPS receptor, since capsular proteins can be recognized and cleaved by phage, leading to exposure of the LPS. CPS is not only a phage receptor, but also plays an important role in bacterial virulence, so bacteria undergo a trade-off between phage resistance and fitness cost. *Acinetobacter baumannii* is able to resist phage infection by reducing the expression of the capsule, which results in diminished fitness *in vivo* and resensitization to complement and antibiotics (32). Phage-resistant *Klebsiella pneumoniae* with deficient CPS synthesis was found to be more sensitive to endocytosis of macrophages (33). In the present study, the CPS-deficient Δ*neuC* mutant may have sacrificed its fitness to maintain phage resistance, which needs to be further studied.

Deletion of the *waaO* or *waaT* gene disrupted the external core structure of the LPS core sugar chain, preventing the binding of phage PNJ1809-36 and abolishing phage plaque formation, while plaques were formed on the Δ*waaW* mutant with the phage. This suggested that the exact binding region of PNJ1809-36 to LPS was on Gal I, which is different from previously reported binding regions in *E. coli* strains, including the terminal Glcα-2Glcα1 or GlcNAcα1-2Glcα1 of LPS (9), the terminal glucose with a β-I,3 glycosidic linkage (34), and the inner core of LPS (35). The difference in adsorption position may lead to a different host spectrum; for example, some phages bind to the highly variable O-antigen, while others bind to the more conserved core polysaccharide of LPS. Thus, these phages have a generally wide host range compared to those able to adsorb O-antigen (36). It has been speculated that the binding region of PNJ1809-36 may also be related to the host range.

It is worth noting that the *neuC* deletion showed a great effect on phage adsorption but only a slight effect on phage plaque formation, whereas *waaO* and *waaT* deletions

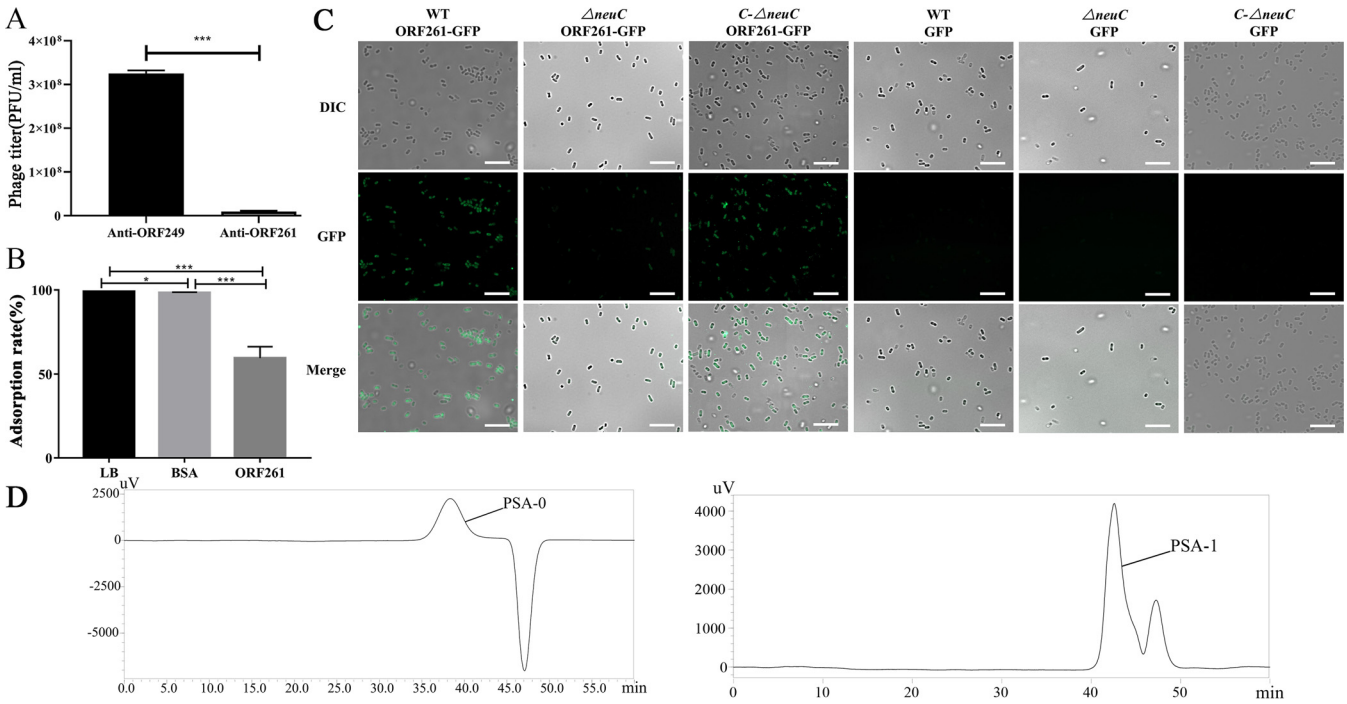

FIG 7 ORF261 binding to the K1 capsule. (A) Antibody blocking assay. The antibody anti-ORF249 was used as a control. The number of plaques formed was counted. (B) Recombinant protein ORF261 competition in the phage adsorption assay. LB medium and BSA were used as controls, and the adsorption rate was set at 100%. All assays were performed in triplicate, and significance was determined by a Student *t* test for comparison between the control group and the treated group. *, $P < 0.05$; **, $P < 0.01$. (C) Binding of protein ORF261 to WT, Δ*neuC* mutant, and complementary C-Δ*neuC* strains. ORF261 with GFP bound easily to WT and complementary strains, but not as well to the Δ*neuC* strain. Proteins containing only GFP could not bind to the strains. (D) HPGPC was used to detect the molecular weight after protein ORF261 was incubated with PSA.PSA-0 or PSA-1 was product of PSA treated with PBS or ORF 261. Other peaks are impurities or solvents.

showed limited effects on phage adsorption but great effects on plaque formation. Thus, we inferred that CPS plays a major role in the initial stage of extensive adsorption of phage, while LPS plays a key role in the later stage of binding. At present, few reports have mentioned LPS and CPS acting as receptors simultaneously.

After identification of the host-encoded receptors, we next found that ORF261, which was predicted to be a depolymerase located in the phage tail, was the RBP interacting with CPS of DE058. Stirm et al. reported that all tested phages that could recognize capsular polysaccharide carry spikes but no tail fibers, indicating that tail spikes are responsible for the recognition of CPS (37), which agrees with our previous results showing that phage PNJ1809-36 was a myovirus carrying spikes but no tail fibers. Stirm also found that K phage not only binds to but also cleaves its receptor (capsular) in order to contact the host membrane for DNA injection (37). Our results are in agreement with Stirm's findings. We found that ORF261 can not only bind but also cleave the CPS.

Based on the above results, we can propose the mode of adsorption and invasion of DE058 by phage PNJ1809-36. First, phage PNJ1809-36 tail protein ORF261 recognizes and adsorbs to the K1 capsule. Second, the K1 capsule is partially degraded, exposing the active site of LPS which is recognized by phage PNJ1809-36 (Fig. 8).

MATERIALS AND METHODS

Bacterial strains, growth conditions, and media. Strains, plasmids and phages used in this study are listed in Table 1. Bacteria were routinely grown at 37°C on solid or in liquid Luria-Bertani (LB) medium supplemented with the appropriate antibiotics: ampicillin (Amp; 100 μg/ml), kanamycin (Kan; 50 μg/ml), nalidixic acid (Nal; 30 μg/ml), and chloramphenicol (Cam; 34 μg/ml).

DNA sequencing and bioinformatics analysis of DE058. Genomic DNA of *E. coli* DE058 was extracted and purified using a bacterial DNA extraction kit (Omega, USA). The genomic DNA was fragmented by ultrasonication, and library preparation was performed using Illumina TruSeq DNA sample prep kits (Illumina, USA). Paired-end sequencing was performed on an Illumina HiSeq 2000 system. The predicted functions of ORFs

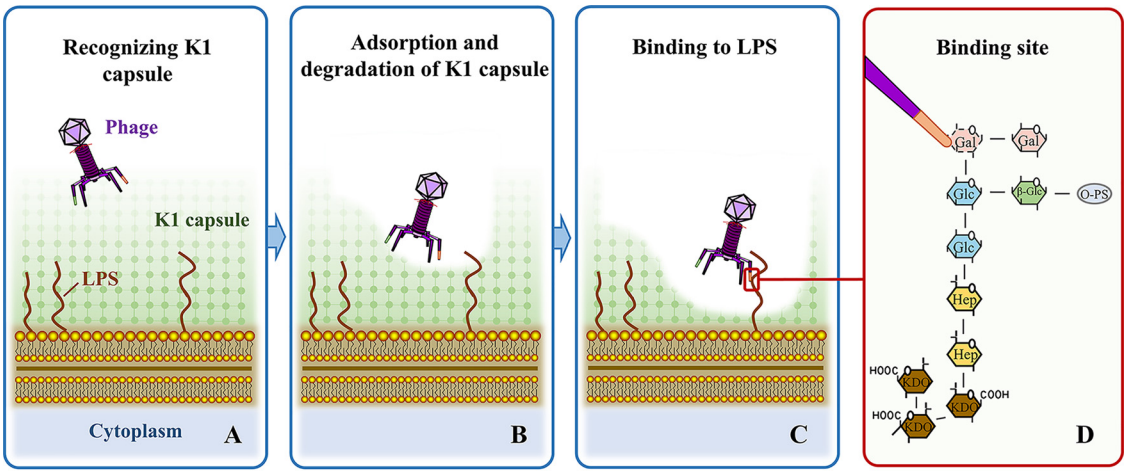

FIG 8 Proposed model of phage PNJ1809-36 recognizing the K1 capsule of *E. coli* DE058. (A) Phage recognizing host bacteria with the K1 capsule. (B) K1 capsule (primary receptor) is recognized and degraded by the tail protein ORF261 of phage. This allows the other tail protein to have access to bind LPS (secondary receptor). (C) Phage PNJ1809-36 recognizes and binds R1 LPS. (D) The other tail protein binds to the penultimate galactose (Gal I) as the specific site.

were then annotated by comparison to the COG database. The type of LPS in DE058 was identified by BLAST DNA sequence in the NCBI database (6).

Phage preparation. Phage PNJ1809-36 was isolated from chicken manure in 2019 and was hosted in APEC DE058. APEC DE058 was grown in LB medium at 37°C to an OD_{600} of 0.6 to 0.8. A mixture of DE058 and PNJ1809-36 in 5 ml of 0.5% of LB agar was poured on the LB agar plate, followed by incubation at 37°C for 6 h. After incubation, plates with confluent lysis were flooded with 5 ml of sterile SM buffer (0.05 M Tris-Cl [pH 7.5], supplemented with 5.8 g NaCl, 2.0 g $MgSO_4s^27H_2O$, and 5 ml of gelatin; 2% [wt/vol] solution), followed by further incubation at 4°C overnight to allow the phage to release. Phage and cell suspensions were harvested and filtered through a sterile 0.22-μm membrane filter. Phage stocks were stored in SM buffer at 4°C.

Transposon mutagenesis and selection of phage-resistant mutants. To establish the mutation library, the donor strain S17-1λpir with transposon plasmid Put-Mini-Tn5-Km was conjugated with the recipient strain DE058 to form a random mutation library. After culture overnight, the mutant was mixed with 50% glycerol, transferred to wells of 96-well plates, and then sealed with sealing membrane and stored at −40°C.

For screening phage-resistant mutants, we used the twice-screen method according to Washizaki et al., with slight modification (7). For initial screening, mutants were cultured in100 μl of LB liquid medium with Kan and Nal antibiotics in a 96-well plate. As a control, wild type DE058 was cultured in 100 μl of LB liquid medium with Nal. The plate was incubated in a shaker at 37°C for 2 h. Then, 100 μl of phage was added to each well of the plate, and 100 μl of LB medium was added to the control well. The OD_{600} value of each well was monitored hourly using a microplate reader (Tecan NanoQuant plate) for 4 h. For the second screening, the colonies not lysed by the phage were judged as suspected phage-resistant mutants and were picked out for further examination by spot assay and double-layer agar experiments.

Genetic manipulations. Transposon insertion sites were identified by Tail-PCR according to the manual of the Genome Walking kit (TaKaRa) (38). AP2 provided by the kit was selected as the forward primer in pre-experiments. Three consecutive reverse specific primers SP1, SP2, and SP3 (GenScript) were designed according to the known sequence of Tn5. The PCR products were sequenced and subjected to BLAST in the NCBI database to determine the insertion site.

Deletion and complementation mutants for selected genes. The Δ*waaO*, Δ*waaT*, Δ*neuC*, and Δ*waaW* deletion mutants were constructed using lambda red recombinase, as described previously (38). The primers were used to amplify a kanamycin resistance cassette using plasmid pKD4 as a template. First, electrocompetent *E. coli* DE058 cells were transformed with the plasmid pKD46. Second, the PCR products were transformed into DE058 with pKD46. Primers (K1, K2, up and down) were used to identify whether the mutants were constructed successfully. Third, plasmid pCP20 was transferred into the mutant to remove the kanamycin resistance gene. Finally, pCP20 was removed by increasing the growth temperature to 42°C, which was confirmed by PCR.

For complementation experiments, pSTV28 was used as the complemented carrier for the genes *waaO*, *waaT*, *neuC*, and *waaW*. The genes were amplified by the primers and then subcloned into pSTV28. pSTV28 was transformed into the corresponding deletion mutants by electroporation. The C-Δ*waaO*, C-Δ*waaT*, C-Δ*neuC*, and C-Δ*waaW* complementary strains were thus successfully constructed (Table 1). The primers are listed in Table 2.

Lysis curve determination. The wild-type, deletion, and complementary strains were cultured to the logarithmic phase, and the OD_{600} value was adjusted to 0.1. A mixture of 100 μl of bacteria and 100 μl of phage was added to the 96-well plate and mixed well (at optimal MOI). As a control, 100 μl of bacteria were mixed with 100 μl of LB medium. The 96-well plate was incubated in the Tecan microplate reader with shaking at 37°C, and the OD_{600} value was monitored every 30 min for 15 h.

TABLE 2 Primers used in this study[a]

Primer	Sequence (5′–3′)
SP1	TTAGTCTGACCATCTCATCTGT
SP2	GCACCTGATTGCCCGACATTAT
SP3	AGCAGACAGTTTTATTGTTCAT
$F_{\triangle waaO}$	AAAGCCACAAAAATCAGGGAAAGAACGATTCGAAAATCGTTGTAATTTCCGGAGAGAAATGTGTAGGCTGGAGCTGCTTCGA
$R_{\triangle waaO}$	TTATCTGCTAAATACGAAAACCGTTCTTTTATAAATTCATTCATTTAACTTTTCTCAATACATATGAATATCCTCCTTAG
$F_{\triangle waaT}$	TAATGAATTATATTTATTATTTTTATTTAAAGATAATAAAATGATATTGAGAAAAGTTAAGTGTAGGCTGGAGCTGCTTCGA
$R_{\triangle waaT}$	GTTATCTTTGTAATAAAATGAGAAGCCGCGATAGCGTATACTTGTAATCATAAGAGTAATCATATGAATATCCTCCTTAG
$F_{\triangle neuC}$	GATTGCATTTTTTTCAACGGGTACATCTATTACACTGGCTCCACGAACACGGCCTTTCTGGTGTAGGCTGGAGCTGCTTCGA
$R_{\triangle neuC}$	GTTGTGGATATAAATATCAATACAACTTCACATACTCACATTCTCCATTCAATGAGTGTTCATATGAATATCCTCCTTAG
K1	CAGTCATAGCCGAATAGCCT
K2	CGGTGCCCTGAATGAACTGC
$up_{\triangle waaO}$	CGCCCCGCTTAAAGACATTA
$down_{\triangle waaO}$	CGCCAGCACCATACAAAAAA
$up_{\triangle waaT}$	GCCATCGTTTCCCGTTTA
$down_{\triangle waaT}$	CTTCTGGAATAATCGGCATATC
$up_{\triangle neuC}$	GTCATAACTGGTGGTACATTC
$down_{\triangle neuC}$	CTTCACATACTCACATTCTCC
$F_{\triangle waaOC}$	TATGACCATGATTACGAATTCTCTTCGATGAATATTGGCCTGAC
$R_{\triangle waaOC}$	CAGGTCGACTCTAGAGGATCCTCATTTTATTATCTTTAAATAAAAATAATAAATATAATT
$F_{\triangle waaTC}$	TATGACCATGATTACGAATTCCTAAGCATAATTTTAAACAAAACAAACC
$R_{\triangle waaTC}$	CAGGTCGACTCTAGAGGATCCTTATTTCTTAAGCTTGTACTTAATTAATGAAGT
$F_{\triangle neuCC}$	TATGACCATGATTACGAATTCCTCTTATGGCAATCTAAATAAAATGTATACTT
$R_{\triangle neuCC}$	CAGGTCGACTCTAGAGGATCCCTAGTCATAACTGGTGGTACATTCCG
$Ft_{\triangle waaO}$	TCAGTGGCATCATCATTCC
$Rt_{\triangle waaO}$	TCAGTAACAACAGCAGCAA
$Ft_{\triangle waaT}$	ATGGTTTGCTGATACTTTCG
$Rt_{\triangle waaT}$	CTGCGGTTATTCCTGACA
$Ft_{\triangle neuC}$	AACCAGAGGAGGAGTTCC
$Rt_{\triangle neuC}$	GCTATCGCAGCATCAATG
Forf261	CAGCAAATGGGTCGCGGATCCATGTCAACTACAATTACTAATTTACCCGA
Rorf261	GCAAGCTTGTCGACGGAGCTCTTATTTACTTTCCAGGGTTGCAAG
Forf249	CAGCAAATGGGTCGCGGATCCATGTCAAGAGTTAAGCACAATATTGACA
Forf249	GCAAGCTTGTCGACGGAGCTCTTACTCGGTAACGTCCACACTAATG
Forf-GFP	CAGCAAATGGGTCGCGGATCCGTTAGCAAAGGCGAGGAACTGT
Rorf-GFP	GTAGTTGACATTTTATACAGTTCATCCATACCCAGGG
Forf261-GFP	CTGTATAAAATGTCAACTACAATTACTAATTTACCCGA
Rorf261-GFP	GCAAGCTTGTCGACGGAGCTCTTATTTACTTTCCAGGGTTGCAAG

[a]All primers were from this study.

Bacterial morphology observation. DE058, Δ*neuC*, and C-Δ*neuC* strains were observed by electron microscopy. Culture lines were drawn on LB agar plates before incubating the plates at 37°C overnight. Doubly deionized H_2O was used to suspend bacterial colonies, which were negatively stained with phosphotungstic acid (2% [wt/vol]) on a copper grid. Cell morphology was observed by an H7650 transmission electron microscope (Hitachi). A capsular staining kit (Solarbio, China) was used for capsular staining. The staining procedures were performed according to the instructions for the kit. The capsule was observed by optical microscopy, as was colony morphology (Leica DM500).

Adsorption assays. The adsorption capacities of wild-type, deletion, and complementary strains were determined. Strains were cultured to the logarithmic phase up to an OD value of 0.5, and then mixed with 500 μl of phage, which was diluted according to the best MOI. After standing at room temperature for 10 min, the mixture was centrifuged at 4°C for 10 min, and the supernatant was taken for plaque counts. The adsorption percentages were calculated using the following formula: [1 − (phage titer of supernatant after cells were removed/phage titer of control reaction mixture without bacterial cells)] × 100% (39).

Inhibitory effect of extra LPS on adsorption. This experiment was carried out according to the Rakhuba et al. method, with slight changes (40). LPS was extracted from DE058 using a lipopolysaccharide extraction kit (iNtRON Biotechnology) and quantified by using a ToxinSensor chromogenic LAL endotoxin assay kit (GenScript). The strain DE058 was cultured to the logarithmic phase, the metabolites were washed out with PBS, and the OD_{600} was adjusted to 0.5. A mixture of 500 μl of purified phage was prepared with 500 μl of bacteria with optimal MOI, and then 10 μl containing different concentrations of LPS was added to this mixture. After 10 min of incubation at room temperature, the mixture was centrifuged at 10,000 × *g* for 10 min at 4°C. The supernatant was diluted for plaque assays to calculate the adsorption rate.

Determination of receptor types by treatment with proteinase K and periodate. The periodate and proteinase K treatment assay were conducted using a previously described method (38, 41). After culture of DE058 to logarithmic phase, the bacteria were collected (5,000 × *g*, 10 min at 4°C), washed with PBS three times, and then suspended to an OD_{600} = 1 bacterial suspension. Bacterial precipitation

was collected after recentrifugation, followed by incubation with 1 ml of different concentrations of periodate or proteinase K for 1 h. The treated bacteria were then washed and used for adsorption determination.

Polyclonal antibody blocking assay. ORF261 and ORF249 (irrelevant tail protein) of phage PNJ1809-36 were cloned into pET-28a, transformed into BL21, and purified by using a HisTrap FF column (GE Healthcare Bio-Sciences AB, Sweden). Polyclonal antibodies against ORF261 and ORF249 were prepared by immunizing New Zealand White rabbits with purified protein.

The blocking effect of antibody on phage adsorption was detected as described in Chen et al. (42). Anti-ORF261 and anti-ORF249 were incubated with phage PNJ1809-36 (10^6 PFU/ml) for 20 min. The host bacterium DE058 was then added to the mixture. The phage adsorption rate was determined by the double-layer agar method.

Protein competition assay. For testing the competitive effect of ORF261, assays were conducting following a previously described method. A volume of 200 μl of purified protein ORF 261 (2 mg/ml) was incubated with 200 μl (42) of DE058 (10^8 CFU/ml) for 30 min at 37°C. DE058 incubating with an equal volume of LB medium or bovine serum albumin (BSA) at 2 mg/ml was used as a control. A total of 100 μl of PNJ1809-36 (10^8 PFU/ml) was added, and the mixture was incubated for 10 min at 37°C. The phage adsorption rates were then tested. Each experiment was performed in triplicate.

Detection of ORF261 binding to CPS of DE058. To detect whether the protein phage tail protein ORF261 could bind to the CPS of DE058, vectors pET-28a-ORF261-GFP and pET-28a-GFP were constructed, and the fluorescent protein was purified by using a HisTrap FF column (GE Healthcare Bio-Sciences AB, Sweden). A volume of 200 μl of purified protein ORF 261-GFP (2 mg/ml) was incubated with 200 μl of DE058 or Δ*neuC* strain (10^8 CFU/ml) for 15 min at 37°C. An equal volume of GFP protein (2 mg/ml) incubated with the strains was used as a control. After incubation, the strains were collected (5,000 × *g*, 10 min at 4°C), washed with PBS three times, and observed under a fluorescence microscope.

HPGPC assays. PSA (Sigma) was incubated with protein ORF261 of phage PNJ1809-36 or imidazole solvent for dissolving protein for 4 h at 37°C. The mixture was prepared at 5 mg/ml and filtered with a 0.22-μm microporous membrane. The molecular weight of the products was determined using a BRT105-104-102 tandem gel column (8 mm × 300 mm), with detection by a Shodex IR 502 refractive index tester. The liquid phase of 0.05 M NaCl was set at a speed of 0.6 ml/min. The column temperature was 40°C.

Ethics statement. All procedures using New Zealand White rabbits were approved by Association for Assessment and Accreditation of Laboratory Animal Care International, and all animal experiments were performed after approval by the Ethical Committee for Animal Experiments of Nanjing Agricultural University (PTA2019024), Nanjing, China.

Data analysis. The data are presented as means ± the standard deviations from a minimum of three independent experiments. Statistical comparisons were carried out using Student *t* tests using GraphPad Prism v7 software. $P \leq 0.05$ was considered significant. Significance is indicated in the figures by asterisks (*, $P < 0.05$; **, $P < 0.01$; ****, $P < 0.0001$).

Data availability. Annotated phage and bacteria genomes were deposited in GenBank and assigned the following accession numbers: MT944117 (PNJ1809-36), JACRRZ000000000 (DE058), JX561091 (*E. coli* phage phAPEC8), DQ832317 (phage rv5), GU070616 (*salmonella* phage PVP-SE1), GU196277.1 (phage K1G), and GU196278.1 (phage K1H).

ACKNOWLEDGMENTS

This study was supported by funds from the National Key R&D Program of China (2019YFC1605400), the Natural Science Foundation of Jiangsu Province (BK20180075), and the Priority Academic Program Development of Jiangsu Higher Education Institutions.

REFERENCES

1. Petrovic Fabijan A, Lin RCY, Ho J, Maddocks S, Ben Zakour NL, Iredell JR, Westmead Bacteriophage Therapy Team. 2020. Safety of bacteriophage therapy in severe *Staphylococcus aureus* infection. Nat Microbiol 5:465–472. https://doi.org/10.1038/s41564-019-0634-z.
2. Dowah ASA, Clokie MRJ. 2018. Review of the nature, diversity and structure of bacteriophage receptor binding proteins that target Gram-positive bacteria. Biophys Rev 10:535–542. https://doi.org/10.1007/s12551-017-0382-3.
3. Mahony J, Cambillau C, van Sinderen D. 2017. Host recognition by lactic acid bacterial phages. FEMS Microbiol Rev 41:S16–S26. https://doi.org/10.1093/femsre/fux019.
4. Bertozzi Silva J, Storms Z, Sauvageau D. 2016. Host receptors for bacteriophage adsorption. FEMS Microbiol Lett 363:fnw002. https://doi.org/10.1093/femsle/fnw002.
5. Latka A, Maciejewska B, Majkowska-Skrobek G, Briers Y, Drulis-Kawa Z. 2017. Bacteriophage-encoded virion-associated enzymes to overcome the carbohydrate barriers during the infection process. Appl Microbiol Biotechnol 101:3103–3119. https://doi.org/10.1007/s00253-017-8224-6.
6. Amor K, Heinrichs DE, Frirdich E, Ziebell K, Johnson RP, Whitfield C. 2000. Distribution of core oligosaccharide types in lipopolysaccharides from *Escherichia coli*. Infect Immun 68:1116–1124. https://doi.org/10.1128/IAI.68.3.1116-1124.2000.
7. Washizaki A, Yonesaki T, Otsuka Y. 2016. Characterization of the interactions between *Escherichia coli* receptors, LPS and OmpC, and bacteriophage T4 long tail fibers. Microbiologyopen 5:1003–1015. https://doi.org/10.1002/mbo3.384.
8. Šimoliūnas E, Vilkaitytė M, Kaliniene L, Zajančkauskaitė A, Kaupinis A, Staniulis J, Valius M, Meškys R, Truncaitė L. 2015. Incomplete LPS core-specific Felix01-like virus vB_EcoM_VpaE1. Viruses 7:6163–6181. https://doi.org/10.3390/v7122932.
9. Sandulache R, Prehm P, Kamp D. 1984. Cell wall receptor for bacteriophage Mu G(+). J Bacteriol 160:299–303. https://doi.org/10.1128/jb.160.1.299-303.1984.
10. Prehm P, Jann B, Jann K, Schmidt G, Stirm S. 1976. On a bacteriophage T3 and T4 receptor region within the cell wall lipopolysaccharide of *Escherichia coli* B. J Mol Biol 101:277–281. https://doi.org/10.1016/0022-2836(76)90377-6.
11. Jann K, Jann B. 1987. Polysaccharide antigens of *Escherichia coli*. Rev Infect Dis 5(Suppl 9):S517–S526. https://doi.org/10.1093/clinids/9.supplement_5.s517.
12. Robbins JB, McCracken GH, Jr, Gotschlich EC, Orskov F, Orskov I, Hanson LA. 1974. *Escherichia coli* K1 capsular polysaccharide associated with neonatal meningitis. N Engl J Med 290:1216–1220. https://doi.org/10.1056/NEJM197405302902202.

13. Scholl D, Rogers S, Adhya S, Merril CR. 2001. Bacteriophage K1-5 encodes two different tail fiber proteins, allowing it to infect and replicate on both K1 and K5 strains of *Escherichia coli*. J Virol 75:2509–2515. https://doi.org/10.1128/JVI.75.6.2509-2515.2001.
14. Fehmel F, Feige U, Niemann H, Stirm S. 1975. *Escherichia coli* capsule bacteriophages. VII. Bacteriophage 29-host capsular polysaccharide interactions. J Virol 16:591–601. https://doi.org/10.1128/JVI.16.3.591-601.1975.
15. Moller-Olsen C, Ross T, Leppard KN, Foisor V, Smith C, Grammatopoulos DK, Sagona AP. 2020. Bacteriophage K1F targets *Escherichia coli* K1 in cerebral endothelial cells and influences the barrier function. Sci Rep 10:8903. https://doi.org/10.1038/s41598-020-65867-4.
16. Machida Y, Miyake K, Hattori K, Yamamoto S, Kawase M, Iijima S. 2000. Structure and function of a novel coliphage-associated sialidase. FEMS Microbiol Lett 182:333–337. https://doi.org/10.1111/j.1574-6968.2000.tb08917.x.
17. Gross RJ, Cheasty T, Rowe B. 1977. Isolation of bacteriophages specific for the K1 polysaccharide antigen of *Escherichia coli*. J Clin Microbiol 6:548–550. https://doi.org/10.1128/jcm.6.6.548-550.1977.
18. Hallenbeck PC, Vimr ER, Yu F, Bassler B, Troy FA. 1987. Purification and properties of a bacteriophage-induced endo-*N*-acetylneuraminidase specific for poly-α-2,8-sialosyl carbohydrate units. J Biol Chem 262:3553–3561. https://doi.org/10.1016/S0021-9258(18)61387-0.
19. Bayer ME, Thurow H, Bayer MH. 1979. Penetration of the polysaccharide capsule of *Escherichia coli* (Bi161/42) by bacteriophage K29. Virology 94:95–118. https://doi.org/10.1016/0042-6822(79)90441-0.
20. Petter JG, Vimr ER. 1993. Complete nucleotide sequence of the bacteriophage K1F tail gene encoding endo-*N*-acylneuraminidase (endo-N) and comparison to an endo-N homolog in bacteriophage PK1E. J Bacteriol 175:4354–4363. https://doi.org/10.1128/jb.175.14.4354-4363.1993.
21. Santos SB, Kropinski AM, Ceyssens PJ, Ackermann HW, Villegas A, Lavigne R, Krylov VN, Carvalho CM, Ferreira EC, Azeredo J. 2011. Genomic and proteomic characterization of the broad-host-range *Salmonella* phage PVP-SE1: creation of a new phage genus. J Virol 85:11265–11273. https://doi.org/10.1128/JVI.01769-10.
22. Tsonos J, Adriaenssens EM, Klumpp J, Hernalsteens JP, Lavigne R, De Greve H. 2012. Complete genome sequence of the novel *Escherichia coli* phage phAPEC8. J Virol 86:13117–13118. https://doi.org/10.1128/JVI.02374-12.
23. Trotereau A, Gonnet M, Viardot A, Lalmanach AC, Guabiraba R, Chanteloup NK, Schouler C. 2017. Complete genome sequences of two *Escherichia coli* phages, vB_EcoM_ ESCO5 and vB_EcoM_ESCO13, which are related to phAPEC8. Genome Announc 5:e10337. https://doi.org/10.1128/genomeA.01337-16.
24. Gong Q, Li Y, Zeng H, Yu P, Qian X, Wang Y, Dai J, Tang F. 2021. Biological characteristics and whole genome analysis of phage PNJ1809-36 target *Escherichia coli* K1. Acta Vet Zootechnica Sinica https://kns.cnki.net/kcms/detail/11.1985.S.20210525.1758.002.html.
25. Johnson JR, O'Bryan TT. 2004. Detection of the *Escherichia coli* group 2 polysaccharide capsule synthesis gene *kpsM* by a rapid and specific PCR-based assay. J Clin Microbiol 42:1773–1776. https://doi.org/10.1128/JCM.42.4.1773-1776.2004.
26. Whitfield C, Roberts IS. 1999. Structure, assembly and regulation of expression of capsules in *Escherichia coli*. Mol Microbiol 31:1307–1319. https://doi.org/10.1046/j.1365-2958.1999.01276.x.
27. Riede I. 1987. Receptor specificity of the short tail fibres (gp12) of T-even type *Escherichia coli* phages. Mol Gen Genet 206:110–115. https://doi.org/10.1007/BF00326544.
28. Heller KJ. 1984. Identification of the phage gene for host receptor specificity by analyzing hybrid phages of T5 and BF23. Virology 139:11–21. https://doi.org/10.1016/0042-6822(84)90325-8.
29. Heller K, Braun V. 1982. Polymannose O-antigens of *Escherichia coli*, the binding sites for the reversible adsorption of bacteriophage $T5^+$ via the L-shaped tail fibers. J Virol 41:222–227. https://doi.org/10.1128/JVI.41.1.222-227.1982.
30. Scholl D, Adhya S, Merril C. 2005. *Escherichia coli* K1's capsule is a barrier to Bacteriophage T7. Appl Environ Microbiol 71:4872–4874. https://doi.org/10.1128/AEM.71.8.4872-4874.2005.
31. Porter NT, Hryckowian AJ, Merrill BD, Fuentes JJ, Gardner JO, Glowacki RWP, Singh S, Crawford RD, Snitkin ES, Sonnenburg JL, Martens EC. 2020. Phase-variable capsular polysaccharides and lipoproteins modify bacteriophage susceptibility in *Bacteroides thetaiotaomicron*. Nat Microbiol 5:1170–1181. https://doi.org/10.1038/s41564-020-0746-5.
32. Gordillo Altamirano F, Forsyth JH, Patwa R, Kostoulias X, Trim M, Subedi D, Archer SK, Morris FC, Oliveira C, Kielty L, Korneev D, O'Bryan MK, Lithgow TJ, Peleg AY, Barr JJ. 2021. Bacteriophage-resistant *Acinetobacter baumannii* are resensitized to antimicrobials. Nat Microbiol 6:157–161. https://doi.org/10.1038/s41564-020-00830-7.
33. Cai R, Wang G, Le S, Wu M, Cheng M, Guo Z, Ji Y, Xi H, Zhao C, Wang X, Xue Y, Wang Z, Zhang H, Fu Y, Sun C, Feng X, Lei L, Yang Y, Ur Rahman S, Liu X, Han W, Gu J. 2019. Three capsular polysaccharide synthesis-related glucosyltransferases, GT-1, GT-2 and WcaJ, are associated with virulence and phage sensitivity of *Klebsiella pneumoniae*. Front Microbiol 10:1189. https://doi.org/10.3389/fmicb.2019.01189.
34. Sandulache R, Prehm P, Expert D, Toussaint A, Kamp D. 1985. The cell wall receptor for bacteriophage Mu G(+) in *Erwinia* and *Escherichia coli* C. FEMS Microbiol Lett 28:307–310. https://doi.org/10.1111/j.1574-6968.1985.tb00811.x.
35. German GJ, Misra R. 2001. The TolC protein of *Escherichia coli* serves as a cell-surface receptor for the newly characterized TLS bacteriophage. J Mol Biol 308:579–585. https://doi.org/10.1006/jmbi.2001.4578.
36. Charbit A, Clement JM, Hofnung M. 1984. Further sequence analysis of the phage lambda receptor site: possible implications for the organization of the LamB protein in *Escherichia coli* K-12. J Mol Biol 175:395–401. https://doi.org/10.1016/0022-2836(84)90355-3.
37. Stirm S, Freund-Molbert E. 1971. *Escherichia coli* capsule bacteriophages. II. Morphology. J Virol 8:330–342. https://doi.org/10.1128/JVI.8.3.330-342.1971.
38. Mutoh N, Furukawa H, Mizushima S. 1978. Role of lipopolysaccharide and outer membrane protein of *Escherichia coli* K-12 in the receptor activity for bacteriophage T4. J Bacteriol 136:693–699. https://doi.org/10.1128/jb.136.2.693-699.1978.
39. Letarov AV, Kulikov EE. 2017. Adsorption of bacteriophages on bacterial cells. Biochemistry (Mosc) 82:1632–1658. https://doi.org/10.1134/S0006297917130053.
40. Rakhuba DV, Kolomiets EI, Dey ES, Novik GI. 2010. Bacteriophage receptors, mechanisms of phage adsorption and penetration into host cell. Pol J Microbiol 59:145–155. https://doi.org/10.33073/pjm-2010-023.
41. Mærk M, Jakobsen ØM, Sletta H, Klinkenberg G, Tøndervik A, Ellingsen TE, Valla S, Ertesvåg H. 2019. Identification of regulatory genes and metabolic processes important for alginate biosynthesis in Azotobacter vinelandii by screening of a transposon insertion mutant library. Front Bioeng Biotechnol 7:475. https://doi.org/10.3389/fbioe.2019.00475.
42. Chen P, Sun H, Ren H, Liu W, Li G, Zhang C. 2020. LamB, OmpC, and the core lipopolysaccharide of *Escherichia coli* K-12 function as receptors of bacteriophage Bp7. J Virol 94:e00325-20. https://doi.org/10.1128/JVI.00325-20.
43. Datsenko KA, Wanner BL. 2000. One-step inactivation of chromosomal genes in *Escherichia coli* K-12 using PCR products. Proc Natl Acad Sci U S A 97:6640–6645. https://doi.org/10.1073/pnas.120163297.